Supporting information

Waugh type $[CoMo_9O_{32}]^{6-}$ cluster with atomically dispersed Co^{IV} for oxygen molecule activation derives from Anderson type $[CoMo_6O_{24}]^{3-}$ anion

Yongdong Chen[a,b], Chaolei Zhang[a,b], Caoping Yang[a], Jiangwei Zhang*[b], Kai Zheng[b], Qihua Fang[b] and Gao Li*[b]

[a] The Center of New Energy Materials and Technology, College of Chemistry and Chemical Engineering, Southwest Petroleum University, Chengdu 610500, China.

[b] State Key Laboratory of Catalysis, Dalian Institute of Chemical Physics, Chinese Academy of Sciences, Dalian 116023, China.

E-mail: jwzhang@dicp.ac.cn (J.W.Z) gaoli@dicp.ac.cn (G.L.).

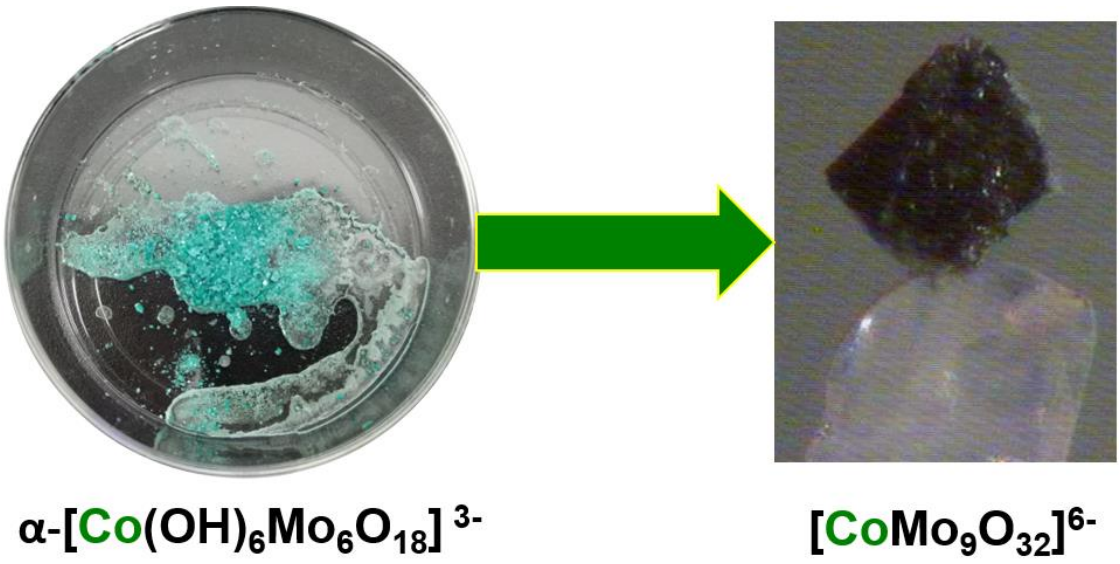

Figure S1. Synthesis of Waugh type $[CoMo_9O_{32}]^{6-}$ cluster derives from Anderson type $[Co(OH)_6Mo_6O_{18}]^{3-}$ and the atrovirens color single crystal view of $[CoMo_9O_{32}]^{6-}$ cluster.

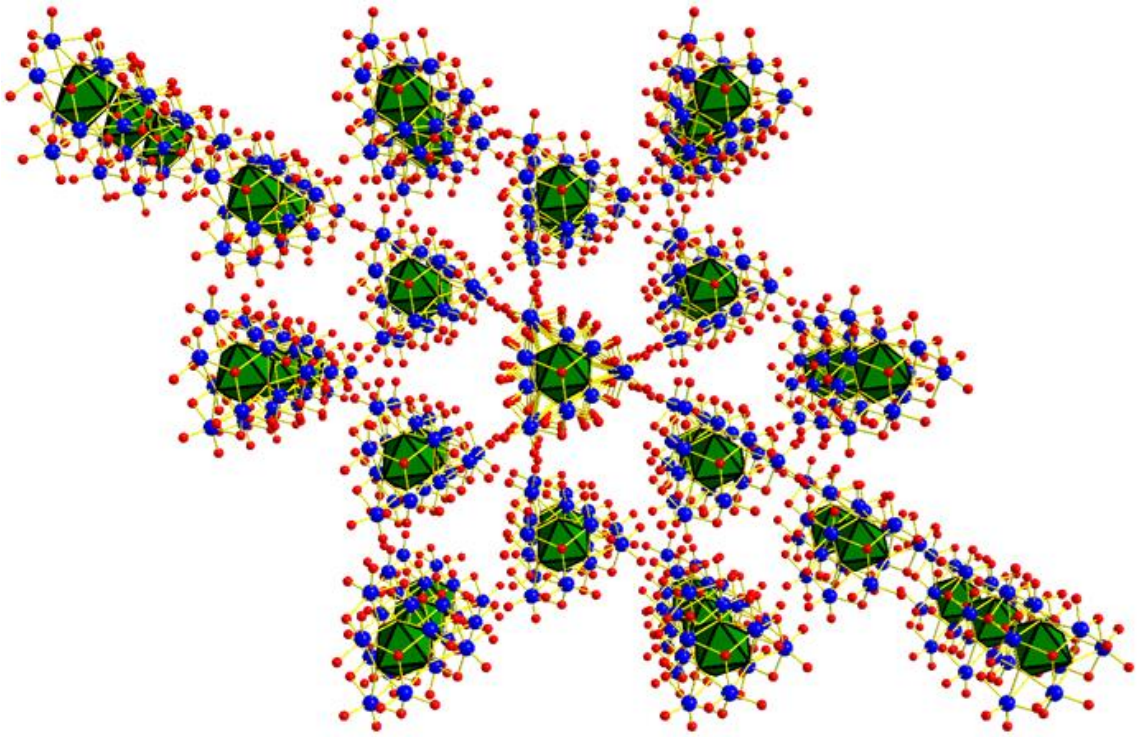

Figure S2a. 3D framework structure of compound **1** packing along *c* axis as quasi 2D material with atomically dispersed Co^{IV} possessed nanoporous in parallel perspective.(countercation NH_4^+ and crystalline water molecule were omitted)

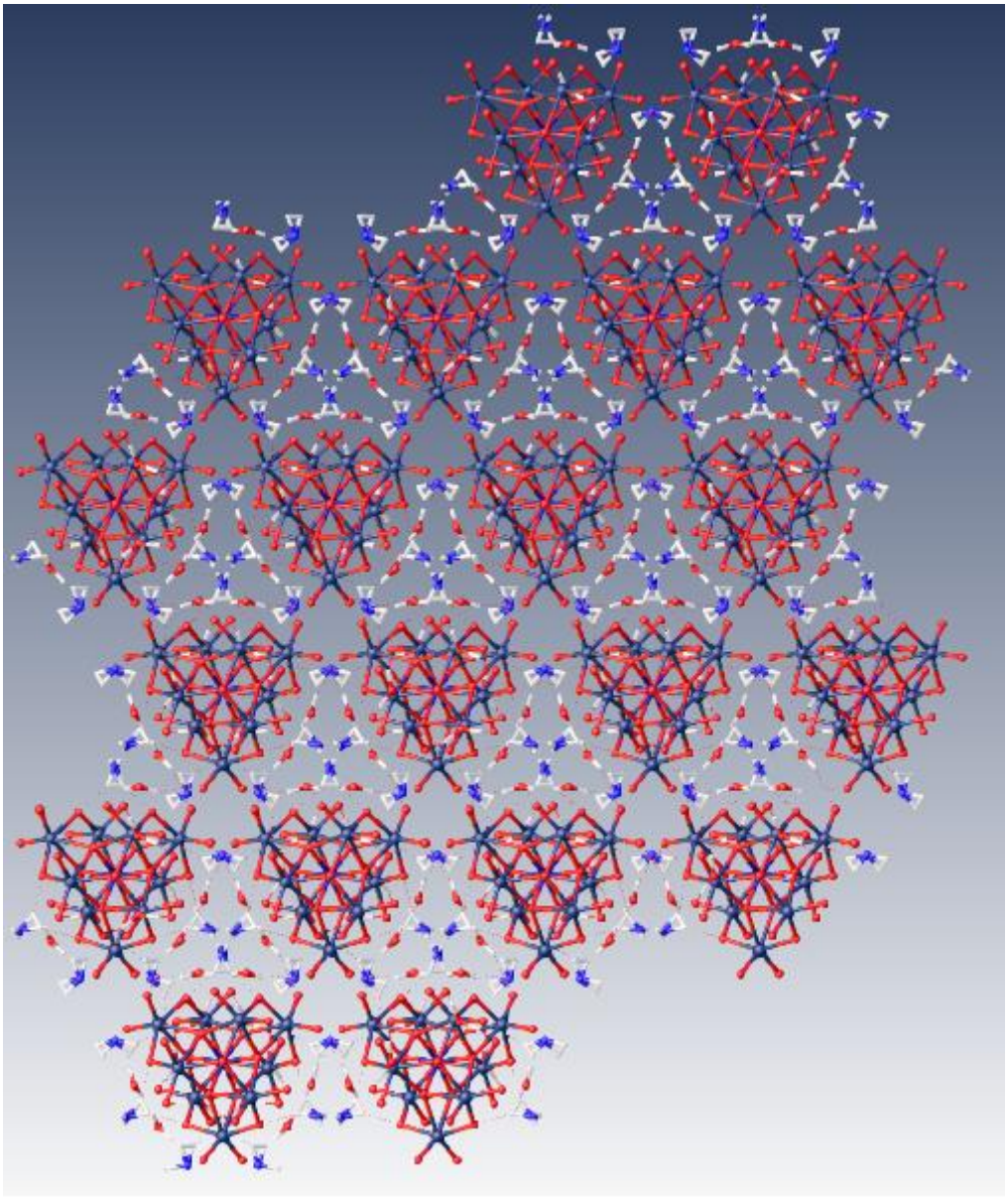

Figure S2b. 3D framework structure of compound **1** packing along *c* axis with countercation NH_4^+ and crystalline water molecule occupied the pore space by hydrogen-bonding interaction with the terminal O atoms of $[CoMo_9O_{32}]^{6-}$ cluster.

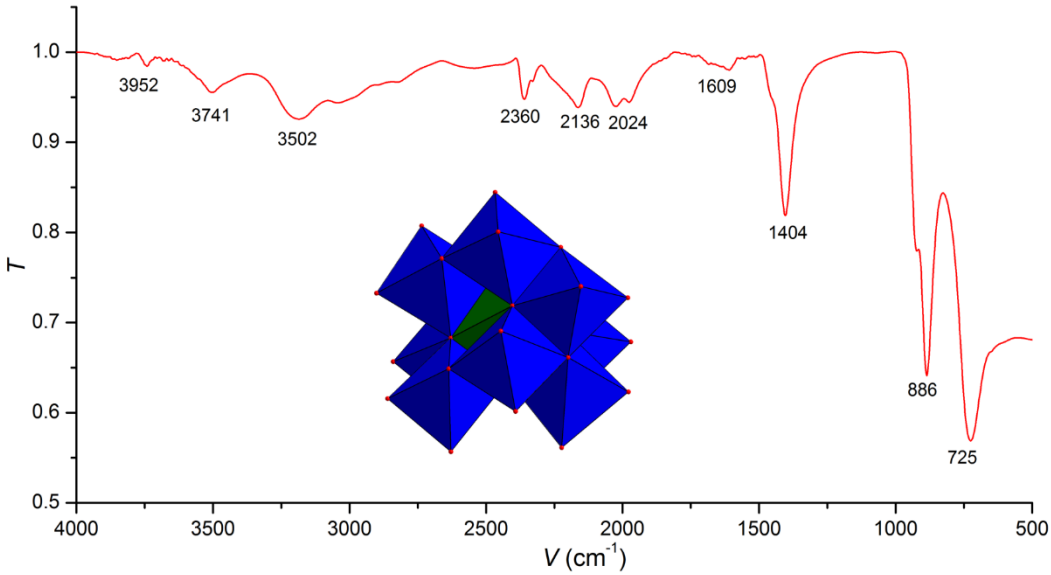

Figure S3. The FT-IR spectrum of compound **1**.

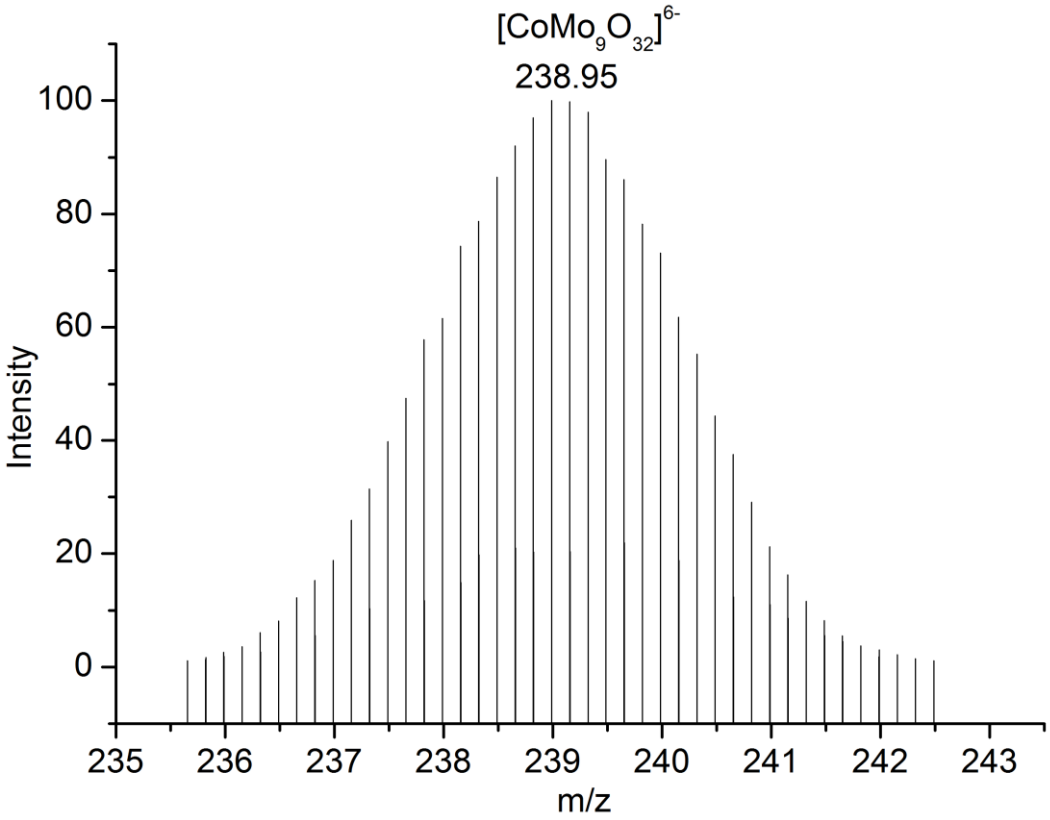

Figure S4. ESI-MS of compound **1**.

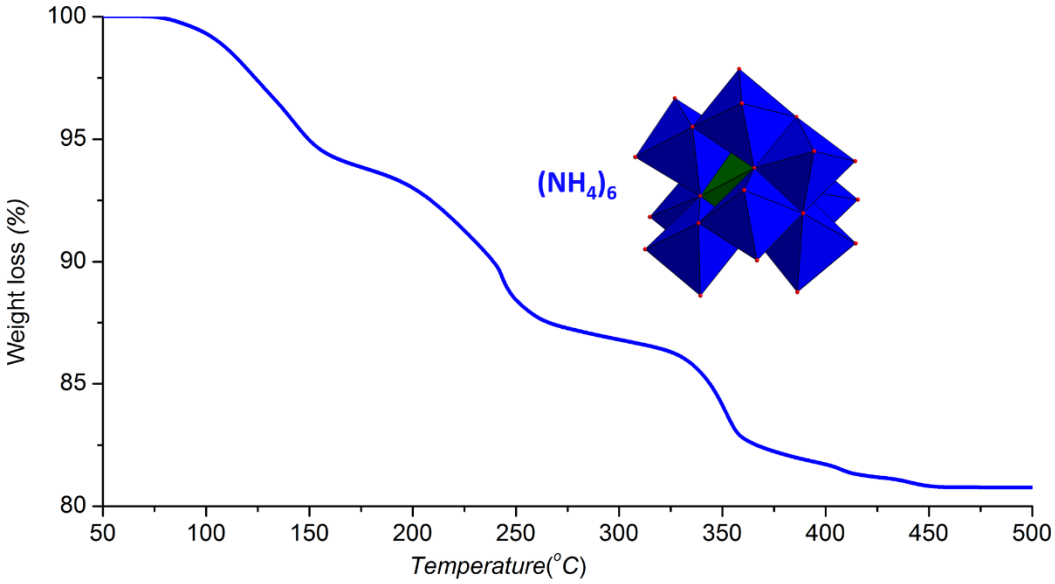

Figure S5. TGA analysis of the $[CoMo_9O_{32}]^{6-}$.

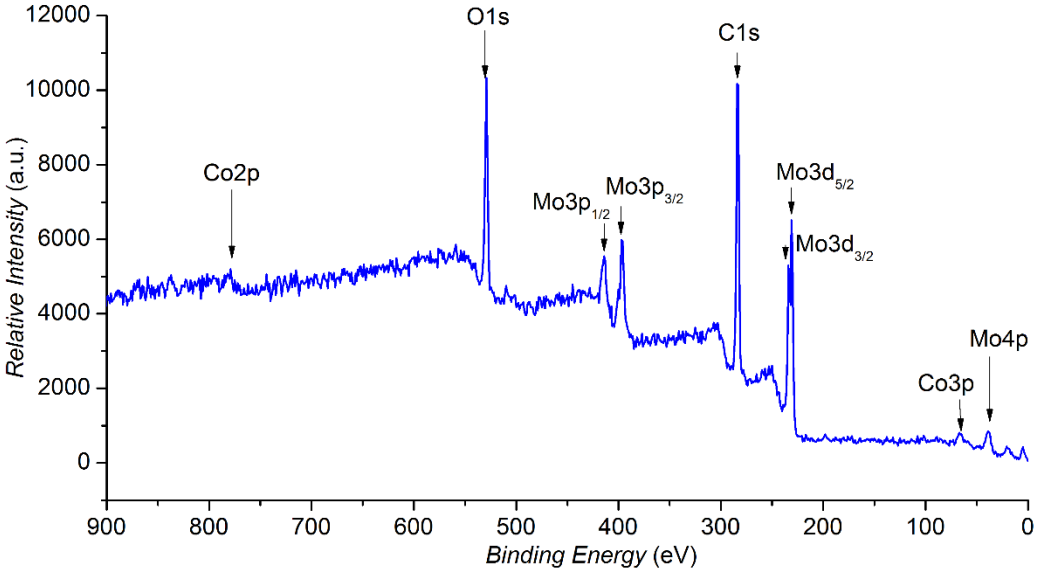

Figure S6. The full XPS spectrum survey of compound **1**

Table S1. Details and results of the BVS calculations.

Subroutine Calc_BVS (JRC-LLB, version: March-2005).

Title: Summary of Bond-Valence calculations for file: $[CoMo_9O_{32}]^{6-}$.cfl

Atom	Coord.	D_aver Sigm	Distort ($x10^{-4}$)	Valence	BVSum (Sigma)
Mo1	6.50	1.9792 (30)	126.021	6.000	6.178 (59)
Mo2	6.00	1.9717 (36)	117.294	6.000	5.915 (72)
Co1	6.00	1.8940 (30)	-0.001	4.000	3.996 (25)
O5	1.00	1.6932 (78)	0.000	-2.000	1.782 (38)
O1	7.00	2.1495 (40)	47.622	-2.000	3.153 (37)
O3	3.00	1.9315 (60)	5.001	-2.000	2.718 (42)
O4	2.00	1.7087 (112)	0.000	-2.000	3.418 (104)
O2	3.00	2.0894 (23)	0.000	-2.000	1.832 (1)
O6	1.00	1.7322 (76)	0.000	-2.000	1.604 (33)

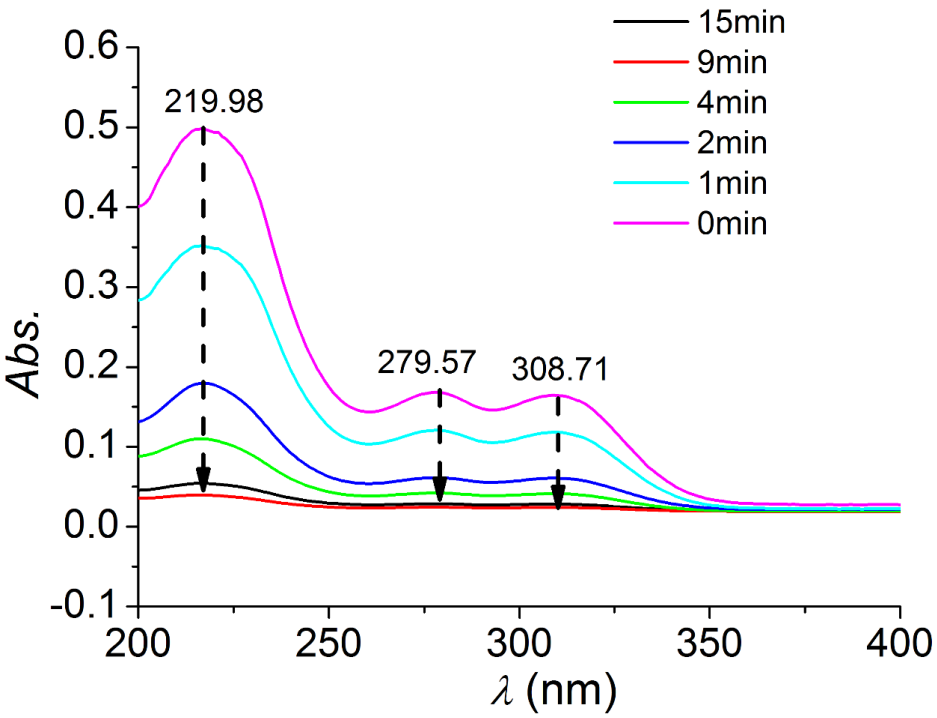

Figure S7. Laser catalytic $^1O_2$ detection was employing DAB as probe and conventional NMB as photosensitizers

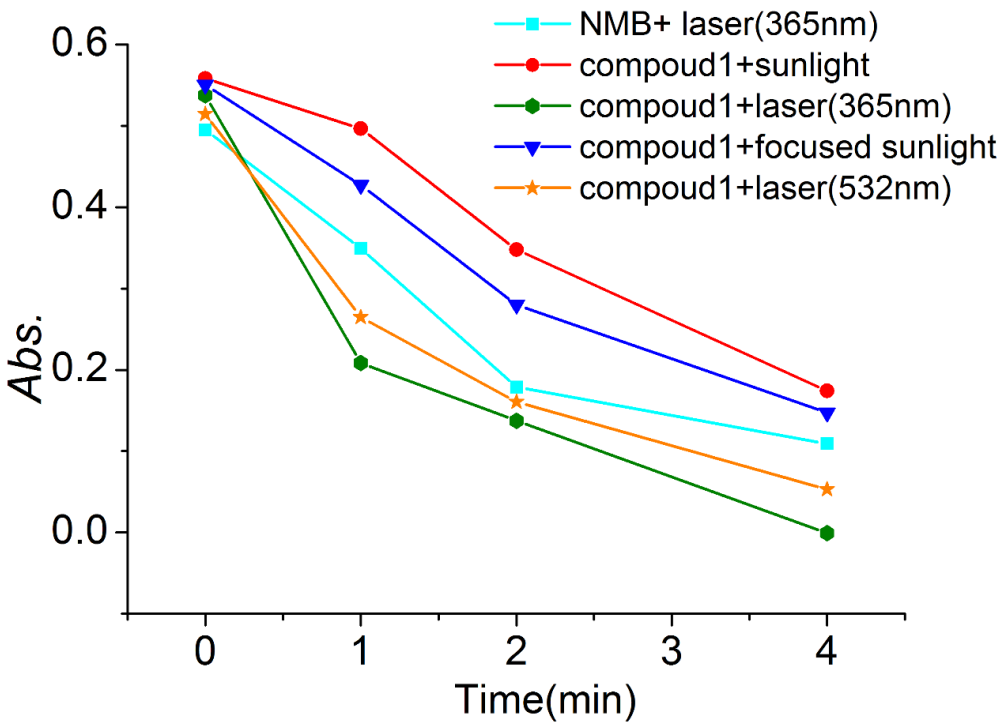

Figure S8. The change in absorbance of chemical probe DAB versus time with variety light sources.

Table S2. The linear fitting parameters of absorption of versus time under different $^1O_2$ generation condition.

Equation	C = Co + R*t				
Weight	No Weighting				
Residual Sum of Squares	1.09E-04	0.00128	0.01101	9.57E-05	0.00353
Pearson's r	-0.99892	-0.97236	-0.93773	-0.99869	-0.97302
		Value	Standard Error		
NMB+ laser(365nm)	Intercept	0.49921	0.00951		
	Slope	-0.15825	0.00737		
compoud1+sunlight	Intercept	0.57293	0.03263		
	Slope	-0.10524	0.02527		
compoud1+laser(365nm)	Intercept	0.49475	0.09579		
	Slope	-0.2003	0.0742		
compoud1+focused sunlight	Intercept	0.5546	0.00893		
	Slope	-0.13512	0.00692		
compoud1+laser(532nm)	Intercept	0.49042	0.05421		
	Slope	-0.17707	0.04199		

Linear fitting equation $C = C_0 + R*t$; where C_o was the original concentration of DAB, R was the $^1O_2$ generation rate, t was time and C was the function of DAB concentration versus time. In this equation C_0 was equals to the intercept while R was equals to the slope.

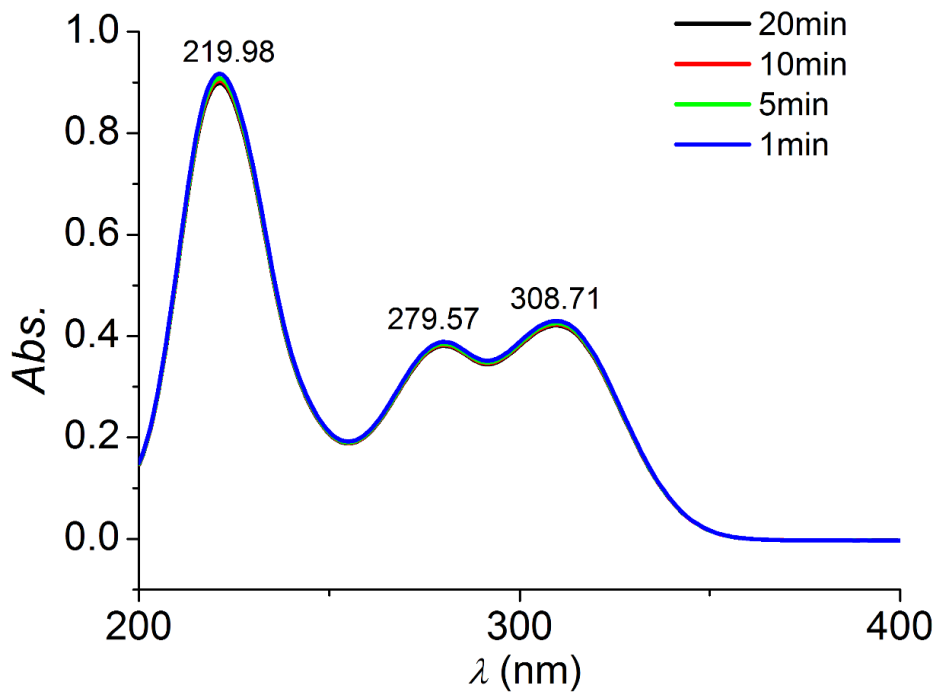

Figure S9. Control experiment of laser catalytic $^1O_2$ detection employing DAB as probe without $[CoMo_9O_{32}]^{6-}$ as photosensitizer with light irradiation (365 nm).